Synchrotron Radiation From Laser-Accelerated Monoenergetic Electrons

Hans-Peter Schlenvoigt, Kerstin Haupt, Alexander Debus, Fabian Budde, Oliver Jäckel, Sebastian Pfotenhauer, Jordan G. Gallacher, Enrico Brunetti, Richard P. Shanks, Samuel M. Wiggins, Dino A. Jaroszynski, Erich Rohwer, and Heinrich Schwoerer

***Abstract*—In this paper, we report on the generation of incoherent synchrotron radiation in the visible spectral range which is produced by laser-accelerated electrons with 55–75-MeV energy as they propagate through an undulator. Simultaneous detection of electron and photon spectra allows for precise comparison between experimental results and undulator theory. First- and second-order undulator radiation was detected. The agreement between experiment and theory and the exclusion of other effects proves that the observed radiation is generated in the undulator. Beyond that, this experiment introduces laser-accelerated electrons into the radio-frequency accelerator domain of synchrotron light sources. This marks a noticeable step toward a new, compact, and brilliant short-wavelength light source.**

***Index Terms*—Accelerators, lasers, synchrotron radiation.**

I. Introduction and Motivation

ULTRASHORT coherent light pulses are an invaluable tool to study the microscopic dynamics of matter. Particularly, femtosecond laser pulses have revolutionized the knowledge of intramolecular and microscopic solid state dynamics in the last two decades, which became possible since the duration of the light pulses is on the order of the characteristic microscopic time scales, and the photon energy is in the range of relevant electronic excitations. Transition states of photoinduced molecular dynamics like isomerization and proton- or energy-transfer reactions can be observed in real time by applying a pump-probe spectroscopy technique with ultrashort laser pulses or even femtosecond laser-generated electron pulses [1]. Serious efforts are made to steer photochemical reactions into desired pathway by controlling the initial coherent motion of vibrational wavepackets [2], [3]. However, the wavelength regime accessible for femtosecond lasers is limited to the near-infrared, visible, and near-ultraviolet spectral range and, thereby, restricts the interaction with matter to electronic transitions and their coupling to the atomic motion.

Shorter wavelengths down to a few nanometers can be generated by synchrotron radiation using electron storage rings or linear accelerators equipped with undulators and, by that, open a more direct view into intermolecular or solid state dynamics through diffraction. This well-established technology grants access to a multitude of beam properties of the produced radiation like wavelength, spectral width, polarization, peak photon numbers, average power, and more. Such light sources topped the performance of conventional X-ray tubes by many orders of magnitude and facilitated time-resolved X-ray diffraction in crystals and recently also of molecules in solution which is of interest for a wide range of interdisciplinary research [4]–[6]. However, the temporal resolution is mostly limited to tens of picoseconds which is significantly larger than for optical pulses and above the desired atomic time scales. Certain technological efforts were undertaken to overcome the limits of synchrotron light sources. In particular, if an undulator is operated in the free-electron-laser mode (FEL), extremely brilliant, ultrashort, polarized, and coherent light pulses are produced. Coherence is obtained by an intrinsically generated modulation of the electron pulses during the interaction with the self-generated light field. This process is called self-amplified spontaneous emission (SASE), which is the basis of all present-day FEL at short wavelengths [7]. Currently constructed free-electron lasers, for example at DESY (Germany) and Berkeley (United States), will have an unprecedented peak brilliance at the nanometer or even Ångstrœm scale at very high average power. They promise a wide applicability, spanning from atomic and cluster physics through temporally resolved structural analysis of complex molecules to plasma physics and even quantum electrodynamics in high external fields [8]. However, today's FEL require several gigaelectronvolts linear electron

Manuscript received November 15, 2007; revised February 11, 2008. This work was supported in part by the Deutsche Forschungsgemeinschaft under Contract TR18 and in part by the Access to Research Infrastructures Activity in the Sixth Framework Program of the EU under Contract RII3-CT-2003-506350, Laserlab Europe. The work of J. G. Gallacher, E. Brunetti, R. P. Shanks, S. M. Wiggins, and D. A. Jaroszynski is supported by the Research Councils U.K. and the EU EuroLEAP NEST under Contract 028514.

H.-P. Schlenvoigt, O. Jäckel, and S. Pfotenhauer are with the Institut für Optik und Quantenelektronik, Friedrich-Schiller-Universität Jena, 07743 Jena, Germany (e-mail: schlenvoigt@ioq.uni-jena.de).

K. Haupt and H. Schwoerer are with the Laser Research Institute, University of Stellenbosch, 7602 Matieland, South Africa, and also with the Institut für Optik und Quantenelektronik, Friedrich-Schiller-Universität Jena, 07743 Jena, Germany.

A. Debus is with Forschungszentrum Dresden-Rossendorf, 01314 Dresden, Germany, and also with the Institut für Optik und Quantenelektronik, Friedrich-Schiller-Universität Jena, 07743 Jena, Germany.

F. Budde is with the Institut für Laser- und Plasmaphysik, Heinrich-Heine-Universität Düsseldorf, 40225 Düsseldorf, Germany, and also with the Institut für Optik und Quantenelektronik, Friedrich-Schiller-Universität Jena, 07743 Jena, Germany.

J. G. Gallacher, E. Brunetti, R. P. Shanks, S. M. Wiggins, and D. A. Jaroszynski are with the Department of Physics, University of Strathclyde, G4 0NG Glasgow, U.K.

E. Rohwer is with the Laser Research Institute, University of Stellenbosch, 7602 Matieland, South Africa.

Color versions of one or more of the figures in this paper are available online at http://ieeexplore.ieee.org.

Digital Object Identifier 10.1109/TPS.2008.927146

0093-3813/$25.00 © 2008 IEEE

accelerators, which are kilometer long due to the maximum energy gain per length of less than 100 MeV/m, which is set by material breakdown of the radio-frequency cavity. In addition, the electron-bunch duration determines the radiation-pulse duration and is still mostly limited to the picosecond level. Special techniques allow for shorter X-ray pulse durations but use only a fraction of the electron pulse.

Bridging the gaps between both fields may become possible with relativistic laser plasma physics. In the late 1970s, a mechanism was predicted to accelerate charged particles with the help of a strongly driven plasma wave [9]. As a driver for such wave, an intense laser pulse or a particle beam is suited [10]. Femtosecond lasers can be used to generate light intensities exceeding 10^{20} W/cm^2 [11]—providing fields strong enough for particle acceleration—which is accomplished with powerful short-pulse laser amplifiers based on the technique of chirped-pulse amplification. During the last decade, many experiments were carried out in order to explore the feasibility of laser–plasma accelerators. Stimulated by particle-in-cell simulations [12], recent experiments have shown that if these laser pulses correctly interact with a self-generated or externally produced underdense plasma, then electrons can be accelerated to energies up to a gigaelectronvolt with a few percent bandwidth and within a well-collimated beam [13]–[16]. The underlying acceleration mechanism is called bubble acceleration: The intense laser pulse strongly drives a longitudinal plasma wave, forming a low-electron-density region (plasma bubble) which is propagating close to the speed of light behind the laser pulse. Some of the plasma electrons are injected into the bubble and accelerated within only a few millimeters to energies of several hundreds of megaelectronvolts [12].

Hence, the energy gain per length for a laser–plasma accelerator is significantly larger than for radio-frequency accelerators, because the acceleration is based on a plasma which in turn has to be avoided in the conventional approach. The electron-pulse duration was measured to be not longer than the laser-pulse duration ($<10^{-13}$ s), and simulations suggest that it might be even shorter due to self-modulation of the laser pulse while it propagates through the plasma [17]. The charge of an electron pulse depends on several parameters, like laser-pulse energy, plasma density, and acceleration regime, and is typically tens to hundreds of picocoulomb for tabletop high-intensity lasers. Thus, the electron-pulse duration of a laser–plasma accelerator is inherently shorter and the peak current higher than for an electron pulse of an RF accelerator.

In this paper, we present the first production of synchrotron radiation from laser-accelerated electrons in more depth as in our previous work [18]. In Section II, we present the experimental methods in detail and discuss several detection and resolution issues. Section III gives a brief overview on synchrotron radiation. In Section IV, we present results of the produced synchrotron radiation as well as characteristics of laser-accelerated electrons. There, we also discuss possible other radiation sources. Finally, in Section V, we present possible future developments for the presented method of producing radiation. We also compare our method with other conventional and laser-based approaches for the production of short-pulse radiation at short wavelengths.

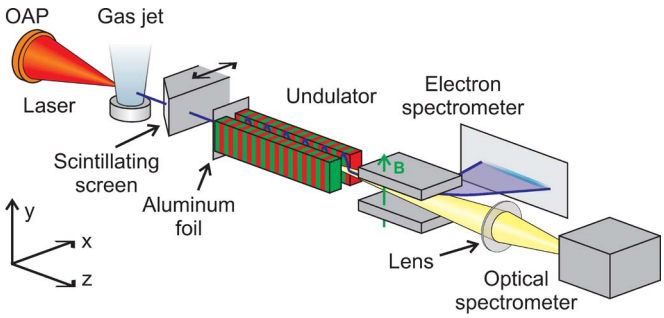

Fig. 1. Setup of the experiment: The main laser pulse is focused by an OAP into a supersonic helium gas jet. The gas becomes fully ionized; the laser pulse undergoes relativistic self-focusing and creates a plasma channel wherein electrons are accelerated to several tens of megaelectronvolts energy. The electron-beam profile may be monitored by a retractable scintillating screen. The electrons propagate through an undulator, producing synchrotron radiation, into a magnetic electron spectrometer where they get dispersed. Radiation is collected with a lens and analyzed by an optical spectrometer. The spectrometer is protected against direct laser and plasma exposure by a thin aluminum foil placed at the undulator entrance.

II. Experimental Methods

The experiment was performed at the Jena high-intensity titanium:sapphire laser JETI. The setup of the experiment consists of a laser-wakefield accelerator as electron source, electron-beam diagnostics, an undulator, an electron spectrometer, and an optical spectrometer. These parts were all aligned along the z-axis (direction of laser propagation). All parts, except the spectrometer, were located inside vacuum chambers. The schematic of the setup is shown in Fig. 1. An essential feature of the experiment is that the acceleration region, the electron spectrum, and the undulator-radiation spectrum were simultaneously recorded for each individual shot.

A. Laser–Plasma Accelerator

In the described experiment, the JETI laser delivered laser pulses at 795-nm central wavelength with an energy of 430 mJ on target within a pulse duration of 85 fs. The laser was focused by an F/6 30° off-axis parabolic mirror (OAP) to a slightly elliptical spot (due to the laser mode) with an area of 95 μm^2 full-width at half-maximum (FWHM), yielding a peak intensity of 5×10^{18} Wcm^{-2}. This corresponds to a normalized vector potential $a_0 = 1.5$, which is defined as $a_0 = eE/(m_0 c\omega)$, where e and m_0 are the electron's charge and rest mass, respectively, E is the amplitude of the electric field, c is the speed of light, and ω is the laser frequency.

At the focal spot, a pulsed supersonic helium gas jet was positioned, generating a super-Gaussian gas-density distribution of 2-mm diameter and a peak gas density of 2×10^{19} cm^{-3}. Since $a_0 > 1$, the laser pulse undergoes ponderomotive and relativistic self-focusing and propagates within a self-generated plasma channel through the fully ionized helium gas. At the selected laser and plasma parameters, the laser pulse experiences a strong longitudinal self-modulation which shortens the pulse and steepens the wake [19]. Electrons are efficiently accelerated to relativistic energies on the order of 50–100 MeV via the bubble regime (also called forced laser-wakefield acceleration) [19], [20]. The self-scattered laser light emitted from the plasma

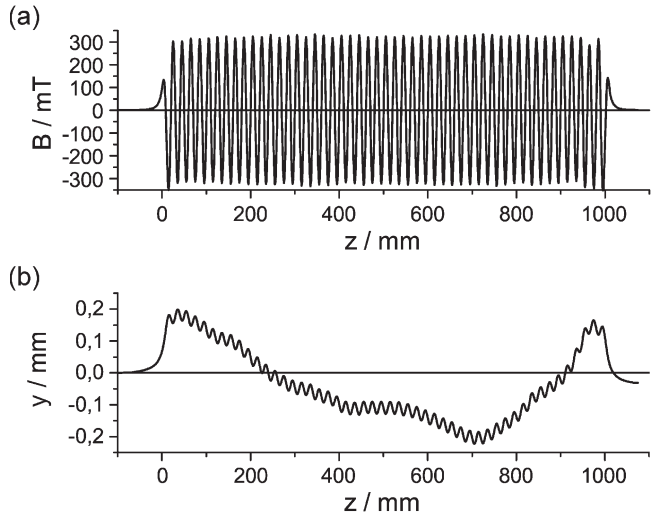

Fig. 2. (a) Magnetic field in x-direction on-axis as function of z. (b) Trajectory of an electron with $\gamma = 100$, injected on-axis. The electron exits parallel to the axis with a negligible offset of 30 μm.

channel perpendicularly to the laser propagation was monitored by a CCD camera equipped with a bandpass filter for fundamental laser frequency for each individual laser shot for online diagnostic and optimization of the laser–plasma interaction and subsequent electron acceleration.

Electron-beam profile images were recorded using a retractable scintillating screen (Konica KR) placed 30 cm behind the focal spot, observed by a CCD camera. The occurrence of well-collimated electron beams was optimized by carefully varying the gas density and the gas-jet position with respect to the laser focus. Besides well-collimated beams, almost every shot showed also a fraction of nondirected electrons. The "center-of-mass" direction of electrons was set to the z-axis by changing the direction of laser incidence on the gas jet while keeping the focus position fixed.

B. Undulator

After removing the scintillating screen, the electrons propagated through an undulator into an electron spectrometer. The undulator is built from permanent magnets in hybrid structure with a period of $\lambda_{\mathrm{u}} = 2$ cm and a length of 1 m ($N = 50$ periods). The distance of the undulator entrance from the gas nozzle was 40 cm. The gap between the magnets was set to 10 mm; the maximum magnetic-field strength on axis was $B = 330$ mT. The undulator parameter, defined as $K = (eB\lambda_{\mathrm{u}})/(2\pi m_0 c)$ amounts to $K = 0.6$. The first and last three periods of the undulator were equipped with ferromagnetic screws allowing fine adjustment of the magnetic field for on-axis injection and on-axis exiting of the electrons. Fig. 2 shows the measured B-field on axis and the path of the electron (equivalent to second field integral) with $\gamma = 100$ through the undulator, injected on-axis. Both the excursion of up to 200 μm and the deviation of 30 μm from the axis at the exit are negligible for electron beams with diameters larger than 1 mm. On-axis exiting is a requirement for subsequent determination of electron energy in the permanent-magnet spectrometer and was therefore taken into consideration at this point.

C. Electron Spectrometer

The electron spectrometer, based on permanent magnets inside an iron yoke, was placed at a distance of 185 cm from the gas jet. The input aperture was 2 cm; however, the full solid angle of acceptance was limited to 7 mrad by the undulator exit. The magnetic-field strength was 720 mT, extending 20 cm in length (z) and 10 cm in width (x), with a gap of 2 cm (y). Scintillating screen (Konica KR) in combination with a CCD camera was used for online electron detection, covering electron energies from 14 to 85 MeV. The screen images were calibrated in terms of measuring charge against an imaging plate (Fuji BAS-MS2025), which could be inserted 15 mm in front of the scintillating screen. Data for the response of the imaging plate and the scintillating screen are taken from [21] and [22], respectively. The spectrometer sensitivity is better than 0.5 pC/MeV. Dispersion was determined by particle tracking based on the 3-D measurements of the magnetic field including fringe effects.

In principle, there is a large energy uncertainty due to the unknown input position and angle of the electrons. The 10-mm-wide undulator exit limits electrons to a maximal deviation of 3.6 mrad from the z-axis. However, a second retractable scintillating screen, similar to the one in front of the undulator, was placed between undulator and electron spectrometer (not shown in Fig. 1). Images from that screen exhibit a focusing effect of the undulator for electrons in the x-direction, which is also the dispersing direction of the electron spectrometer (cf. Fig. 1). The screen images show an average localization of electrons within a range of 2 mm from the z-axis, which is in reasonable accordance with particle-tracking simulations of the undulator, proving this focusing effect. The resulting electron-spectrometer-energy uncertainty is smaller than 10%. Note that there was no possibility for simultaneous detection of electron-beam profiles, electron-energy spectra, and radiation spectra. The scintillating screen blocks the undulator radiation and scatters the electron beam. In addition, we refrained from smaller input apertures for the electron spectrometer because that reduced the radiation signal dramatically.

However, for a well-collimated and monoenergetic electron bunch, the discrimination between beam divergence and energy spread may be accomplished by measuring the electron beam divergence along the y-direction (nondispersive) and assuming the same divergence along the x-direction. This assumption is reasonable, since the electron-beam profiles show only little asymmetry for such bunches. Thus, despite the mentioned uncertainty of the peak-energy position, the spectral width can be determined within 2%.

D. Optical Detection System

Undulator radiation was collected and focused into the entrance slit plane of a symmetrical 200-mm Czerny–Turner spectrometer. A thermoelectrically cooled CCD camera (Andor DO-420 BN) was used as detector, shielded with lead against X-rays from electron stopping in the vacuum-vessel walls. The 26.6×6.7-mm^2 CCD chip (1024×256 pixels) was operated in hardware-binning mode, merging arrays of

8×12 pixels together to superpixels which is useful, since there is no need for high spectral resolution, and thermal noise and quantization errors are reduced. The spectral range was set to 560–990-nm; wavelength calibration was accomplished with a Hg-vapor lamp. The spectrometer efficiency was carefully calibrated by means of a calibrated visible light source. Due to the intrinsically parallel photon detection within each CCD pixel, saturation of the signal from the ultrashort pulses did not occur. In order to screen the optical spectrometer against direct exposure with laser and plasma light, a 15-μm-thick aluminum foil was placed in front of the undulator.

Raytracing simulations of the optical system show that the collection angle for undulator radiation is about 2 mrad, which is significantly smaller than from simple geometrical estimation. The light source to be imaged is extended 1 m in depth (demands an extremely high depth of focus), which is difficult to image onto the slit plane without significant loss of flux. In the experiment, the longitudinal center of the undulator was imaged onto the slit plane, resulting in a maximum of intensity and average image quality.

III. Undulator Radiation

The relativistic laser-accelerated electrons undergo oscillations in the undulator perpendicular to the magnetic field and the propagation direction and, therefore, emit polarized radiation. Due to the relativistic movement, the emission is anisotropic and peaked in forward direction. The wavelength λ of the emitted light is mainly determined by the undulator period λ_u, and the electron energy $E_\mathrm{e} = \gamma m_0 c^2$ (γ is the Lorentz factor) and to second order by the undulator parameter K, determining the amplitude of the oscillatory motion. Furthermore, the emission wavelength depends on the angle of emission ϑ with respect to the propagation direction [23]

$$\lambda = \frac{\lambda_\mathrm{u}}{2\gamma^2 n} \cdot \left(1 + \frac{K^2}{2} + \gamma^2 \vartheta^2\right) \tag{1}$$

where n is the harmonic order of the emission. For $K < 1$, as in the case of our undulator, the emitted wavelength in forward direction is approximately $\lambda \approx \lambda_\mathrm{u}/2\gamma^2$. For electron energies around 55–75 MeV, the wavelength of fundamental radiation emitted with our undulator ($\lambda_\mathrm{u} = 2$ cm) is in the visible spectral range (560–990 nm). The natural linewidth of undulator radiation is given by the number of oscillations which is equal to the number of periods N: $\Delta\lambda_\mathrm{nat}/\lambda = 1/N$. This amounts to 2% in our case. Furthermore, due to the angular variation of the emitted wavelength, the observed spectrum also strongly depends on the solid angle of observation and electron-beam divergence.

The energy E_u emitted by a single electron for fundamental undulator radiation ($n = 1$) increases linearly with the number of periods N and quadratically with the electron energy γ [23]

$$E_\mathrm{u} = \frac{\pi e}{3\epsilon_0} \frac{N\gamma^2 K^2 e}{\lambda_\mathrm{u}(1 + K^2/2)^2} \tag{2}$$

TABLE I
Properties of Laser-Accelerated Electrons, Determined (Top) From Electron-Beam Profile Images and (Below) From the Electron Spectrometer

Property	Quantity
relative frequency of well-collimated beams	0.7 per shot
divergence of well-collimated beams	3 - 7 mrad
average divergence of electrons	30 mrad
mean variation of well-collimated beams	60 mrad
rel. frequency monoenergetic spectra	0.25 per shot
predominant charge of monoenergetic peak	10 pC -20 pC
predominant peak energy	40 MeV - 45 MeV

where ϵ_0 is the permittivity of free space. Considering the mean photon energy $E_\mathrm{ph} = hc/\lambda$, one can estimate the number of emitted photons per electron to be $N_\mathrm{ph} = E_\mathrm{u}/E_\mathrm{ph}$.

For more than one electron, the emission can superimpose coherently or incoherently. An incoherent superposition takes place if the electrons are distributed over a distance significantly larger than the emitted wavelength λ. In that case, the number of emitted photons scales linearly with the number of electrons N_e, respectively, the total charge in the pulse. This is the situation of the experimental conditions described here. In the vice-versa case of a coherent superposition, which is possible if all electrons are bunched within a range significantly shorter than the wavelength (or become microbunched as inside a FEL), the emission scales with the number of electrons squared N_e^2, until saturation sets in due to a significant energy exchange from the electron to the radiation.

For this experiment, accurate calculations of incoherent radiation spectra are necessary which regard the collection angle and electron-energy spectrum. Undulator-radiation spectra were computed as follows. For the given magnetic field, the trajectory and the Lienard–Wiechert-potentials are calculated with dependence of the electron energy. Integrating over the solid angle of detection and convolving with the electron spectrum, the radiation spectrum is obtained for arbitrary electron spectra [24]. By that, we were able to compare measured radiation spectra with simulations based on measured electron spectra.

IV. Results

A. Electron Beams

The laser-driven electron source was optimized prior to shots through the undulator and measurements of optical radiation. Properties of the produced electron beams with relevance to this experiment are given in Table I.

Observations of the electron-beam profiles with the scintillating screen show two types of electron beams: a weak and divergent electron "cloud" which is observed almost every shot. Well-collimated electron beams occur quite often but with significant fluctuations around their average direction and are superimposed to the cloud. The probability that a well-collimated beam propagates through the undulator is about one in hundred shots. From previous experiments [13]–[16], [19], [25], we assumed only well-collimated beams to give narrowband spectra. Surprisingly, the electron spectra show one out of four shots having narrowband features in the full-detection range of the electron spectrometer from 20 to 80 MeV. That must be explained by the cloudy fraction of electrons

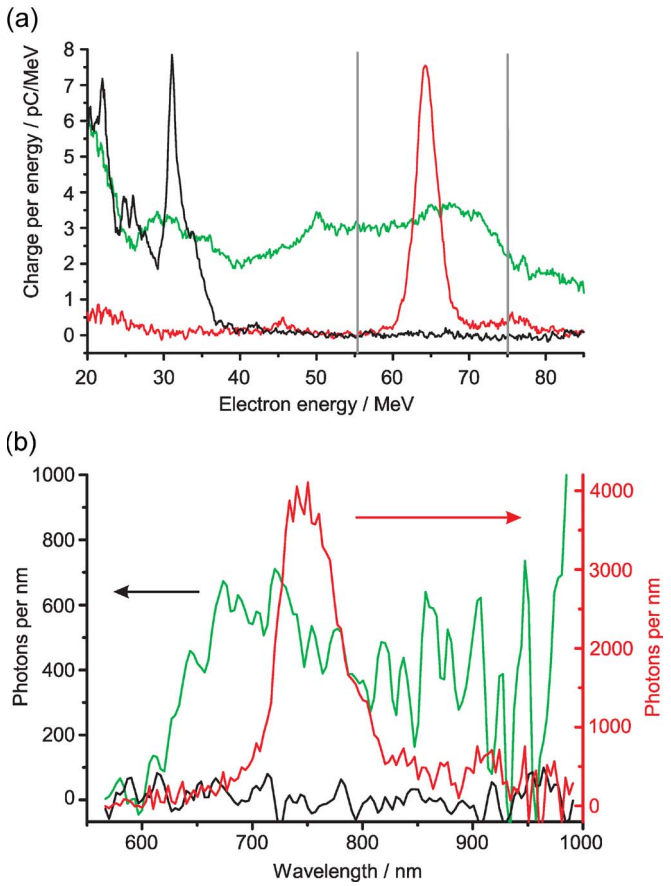

Fig. 3. (a) Electron spectra and (b) corresponding optical-radiation spectra for three shots. The vertical gray bars in graph (a) indicate the range of electron energies (55–75 MeV) where undulator radiation would be within the range of the optical spectrometer (560–990 nm). The right-hand-side ordinate in graph (b) is for the red shot.

present in every shot, which were, so far, expected to be broadband. The narrowband peak energies vary between 20 and 70 MeV with a maximum in the range of 40–45 MeV, and the charge of such peak is mostly below 40 pC. There are considerable fluctuations of electron-beam position and electron energy spectrum, induced by the little fluctuations of the gas jet, laser-beam profile, and pulse energy, but boosted by the highly nonlinear acceleration regime. Despite this, the parameters are very encouraging for a further use of such electron beams like passing through an undulator. Results of undulator radiation are presented in the following.

B. Undulator Radiation

Fig. 3 shows three examples of pairs of electron spectra (top) and corresponding optical-radiation spectra (bottom, same color means same shot). The gray vertical bars at the electron spectra indicate the energy range where undulator radiation would be expected within the spectral range of the optical spectrometer.

The red electron spectrum is peaked at 64 MeV, right within the energy range of interest, and has almost no electrons at lower energies. We observe a very strong peak at 740 nm with the optical spectrometer (right-hand-side ordinate due to

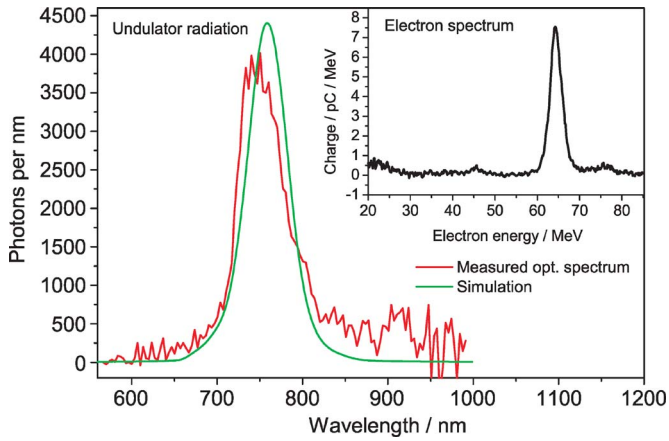

Fig. 4. (Red) Measured optical-radiation spectrum and (green) simulated undulator-radiation spectrum which was calculated from (inset) the corresponding electron spectrum.

rescaling with the other shots). The peak positions agree very well with (1).

The green electron spectrum is broadband, however, with a particular spectral shape in the detection range: slowly increasing toward a slight peak at 67 MeV and then a faster decrease. The same spectral shape with a corresponding peak position is observed with the optical spectrometer.

The black electron spectrum shows a peak as strong as the red one but at 30 MeV electron energy and no electrons for energies above 40 MeV. Hence, the radiation is expected around $\lambda \approx 3\ \mu$m, beyond the detection range of the optical spectrometer. Indeed, no optical radiation was detected.

A more precise data evaluation was carried out with the help of simulations. Fig. 4 shows again the red displayed shot from Fig. 3. It shows as inset that the electron spectrum, which is peaked at 64 MeV, has a width of 3.4 MeV (FWHM) and contains a charge of 10 pC. Optical radiation (red) is peaked at 740 nm and has a bandwidth of 55 nm. The total number of photons within the linewidth is determined to be 280 000. Based on the electron spectrum, the undulator-radiation spectrum was simulated as described earlier and is shown as green line in Fig. 4. It shows an excellent agreement with the measured undulator radiation. The slight offset of the peak positions is negligible in consideration of the uncertainty for electron-spectrum peak positions, and spectral width and photon numbers are in perfect agreement.

Fig. 5 shows the correlation between electron-spectrum peak energy and optical-radiation peak wavelength. For each shot having a peak with a sufficient charge (spectral intensity greater than 1 pC/MeV) within the energy interval of 55–75 MeV, a peaked undulator-radiation spectrum was measured, and the peak wavelengths correspond very well to the expected wavelengths. Shots generating electron pulses with energies below 55 MeV—corresponding to undulator radiation beyond the optical spectrometer's range—produced no signal on the optical spectrometer, with the exception of a few shots with peak energies between 40 and 50 MeV and with very high charge within the peak. These shots produced a very small signal on the optical spectrometer at wavelengths corresponding to the second harmonic of undulator radiation [$n = 2$ in (1)]. For

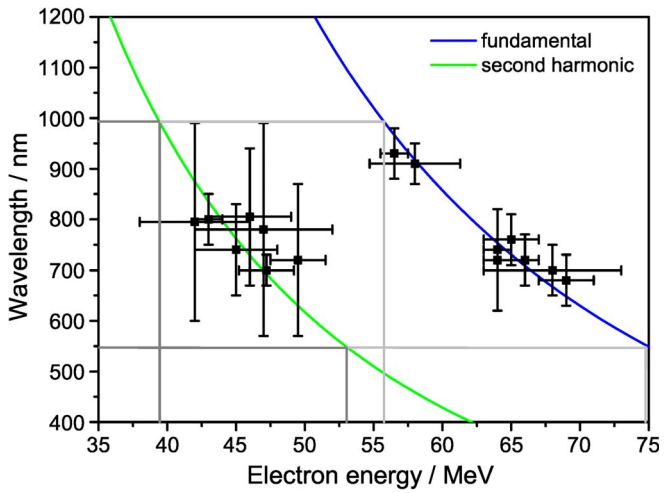

Fig. 5. Correlation between measured electron spectra peak energies and undulator-radiation spectra peak wavelengths. The solid lines display the theoretical relation between electron energy and undulator-radiation wavelength according to (1) for (blue, $n = 1$) the fundamental and (green, $n = 2$) second harmonic. The gray bars arise from the detection range for optical radiation (560–990 nm) and guide to ranges for electron energies where electrons should produce an optical signal. Note: The error bars do not show an error in the sense of an uncertainty but the width of the electron and optical spectrometer signal, respectively.

these shots, the electron spectral intensity had to be above 7 pC/MeV in order to produce a detectable optical signal, which were indeed very faint with a typical signal-to-noise ratio < 2. This behavior is consistent with simulations of undulator radiation—based on the actual undulator parameters—which exhibit an intensity ratio of 10 : 1 for fundamental to second-harmonic undulator radiation.

All shots shown in Fig. 5 fit well whether to fundamental undulator radiation (blue line) or second harmonic (green line). Over and above, it must be noted that there were no shots with an optical signal but without a corresponding electron spectrum, and vice versa.

Further sources of light, which possibly could have been detected by the spectrometer, are excluded as follows. Direct laser light, plasma emission, and transition radiation from the plasma–vacuum boundary are completely blocked by the aluminum foil in front of the undulator. Furthermore, tiny leakages in the foil would easily be uncovered by the laser light as the most intense fraction. Laser light would be observed and, thus, easily identified via the constant spectrum at 800 nm.

In fact, only transition radiation from the foil–vacuum boundary is a conceivable source of interfering light. Transition radiation occurs if an electron pulse crosses an interface where the dielectric function varies. The interaction of the current with the boundary generates broadband radiation. However, for wavelengths longer than the bunch length, a coherent superposition results and increases the intensity for such wavelengths. For coherent transition radiation with wavelengths detectable by our spectrometer, the bunch duration would have to be shorter than 3 fs. Furthermore, if there is a periodical modulation on the longitudinal structure similar to microbunching in a FEL, such coherent transition radiation will be produced as well, leading to increased intensities at wavelengths given by the periodicity. Recently, coherent transition radiation from laser-accelerated electrons at wavelengths from 400 nm–1 μm was observed [26]. The laser pulse interacts with the laser-accelerated electrons and imprints its periodicity. But this impression is washed out with increasing distance between the laser–plasma accelerator and metal foil due to space-charge effects of the electron bunch. Referring to [26], in our case of 400-mm distance between aluminum foil and acceleration region, the imprint of the laser is faded. Thus, in the wavelength range of our spectrometer, only incoherent broadband transition radiation may be produced, unable to explain neither the correlation between electron spectrum peak energies and optical spectrum peak wavelengths for various shots (Figs. 3 and 5) nor the agreement between simulated and measured spectrum (Fig. 4). In addition, in contrast to undulator radiation, transition radiation is emitted into lobes separated by an angle $\vartheta \sim 1/\gamma$ with zero intensity on axis. Hence, the lens collects transition radiation around its intensity minimum, and the imaging of this source onto the entrance slit plane of the optical spectrometer is worse than for undulator radiation, and the overall signal will be very small. All in all, in fact, we did not observe an optical background signal. In conclusion, we show strong evidence that the observed narrowband radiation is indeed generated by electrons wiggling through the undulator.

V. Conclusion and Perspectives

As aforementioned, electron acceleration with high-intensity lasers has made rapidly significant progress within the last five years. Stimulated by 3-D particle in cell simulations [12], the acceleration of narrowband electrons through the bubble-acceleration mechanism was experimentally demonstrated in 2004 [13]–[15]. A maximum electron energy of 1 GeV was achieved in 2006 by replacing the gas jet by a 3-cm-long gas-filled capillary discharge waveguide [16]. Finally, the reproducibility of electron energy and charge in the pulse was improved and became controllable by triggering the electron injection into the accelerating plasma wave by means of a counterpropagating laser pulse [25]. The authors have no doubt that this worldwide development will rapidly proceed in the next few years toward predictable electron pulses in the giga-electronvolts range with percent energy width, still generated by present-day tabletop high-intensity lasers.

In order to improve the reliability of producing synchrotron radiation from laser-accelerated electrons as described in this paper, it is necessary to have a stable electron beam with very good collimation. Furthermore, predictable electron energies and very small energy spread would be desired. The use of capillary discharge waveguides [16], as well as the triggered injection by a counterpropagating laser pulse[25], give stable electron beams with very little divergence. However, the use of a counterpropagating laser beam is difficult and complicates the setup together with an undulator. The use of a capillary discharge waveguide seems more promising, since the divergence is even smaller than with a counterpropagating laser beam (2 mrad instead of 6 mrad), but the electron-beam energy is not as selectable as with triggered injection.

Due to the favorable $1/\gamma^2$ scaling of the undulator radiation (1), ultrashort incoherent light pulses in the UV and soft X-ray

spectral range will soon be produced by the method described in this paper. Considering the laser-produced 1 GeV electron beam [16] in combination with our undulator ($\lambda_u = 2$ cm), (1) predicts radiation with 2.5-nm wavelength or 500-eV photon energy, respectively.

The generation of coherent undulator radiation is more challenging, since it requires electron pulses (or pulse structures) shorter than the emitted wavelength. With today's laser-accelerated electrons, this might be possible in the infrared spectral range using undulators with long period. This is possible since the electron pulses are effectively prebunched in order to produce coherent synchrotron radiation [27]. However, in the UV or even X-ray region, one has to rely on the SASE process [28]. The core of the SASE process is the interaction between the electron pulse and its own undulator radiation, which leads to a spatial modulation of the electron density and, finally, to a break-up of the electron pulse into a trace of equidistant short pulses; each of them then emitting coherent light. This requires high-quality electron beams in combination with long and highly engineered undulators, since this process starts from spontaneous synchrotron radiation and takes a certain length (gain length) in order to modulate the electron pulse. The gain length is determined by the inverse of the Pierce parameter ρ, which may be written as follows [27], [29]:

$$\rho \sim \frac{1}{\gamma}\left(\frac{\lambda_u^2}{\sigma_x \sigma_y}\frac{I_p}{I_A}\right)^{1/3} \tag{3}$$

where σ_x and σ_y are the beam diameters in x- and y-directions, respectively, I_p is the peak current, and $I_A = 17$ kA is the Alfven current. In order to reduce the gain length and therewith the undulator length, the Pierce parameter has to be large. Usually, the beam size is reduced by focusing the electron beam, which requires electron beams with extremely low emittance. However, as shown in (3), the gain length may also be reduced with a high current of the electron beam. Due to the ultrashort pulse durations of electron pulses from laser–plasma accelerators, the peak current will be much higher as from RF accelerators. Hence, laser–plasma-based electron accelerators might be ideal drivers for FEL [29], [30].

An additional advantageous aspect of a purely laser-driven undulator radiation is the temporal coupling of the laser light and the undulator radiation. Each time-resolved experiment relies on the pump-probe technique. Microscopic dynamics are started to be an ultrashort pump pulse and are probed by a second ultrashort pulse after a certain time delay. Without ultrashort pulses, no sufficient time resolution would be obtained. Thus, a laser-based source is perfectly suited. Splitting and delaying optical pulses may be accomplished with subfemtosecond time resolution and perfect reproducibility. Up to now, one of the two pulses is typically a femtosecond laser pulse, externally coupled to the accelerator RF source or with a separate delay measurement for each shot. That would be overcome with a laser-based synchrotron source. Furthermore, there are possibilities to convert the laser pulse into a second laser-driven electron pulse, X-ray pulse [31], [32], or even ion pulse [33], [34]. The second pulse just has to be amplified with a second arm of the laser system, and the multitude of laser-driven sources with all their unique properties and exotic states of matter are accessible as pump or probe pulse.

Other laser-based radiation at short wavelengths are Betatron radiation, Thomson-Backscattering, and X-ray line emission. Betatron radiation [35] from laser-produced plasmas is generated by laser-accelerated electron, which undergo a transverse oscillation in the plasma wake. Thus, the implementation is quite easy, but the radiation strongly depends on the transverse excursion of the electrons and their energy. Hence, the radiation is broadband, and this method turned out to be rather a diagnostic tool for electron acceleration [36]. For Thomson-Backscattering [20], the static magnetic field is replaced by a counterpropagating electric field of a laser pulse. This allows again for ultrashort narrowband-polarized pulses and wavelength tuning and has the advantage that, for the same electron energy, the photon energies are higher as for an undulator because the undulator period is now submicrometer [37]. However, the experimental setup is difficult to handle [20]. X-ray line emission [38] is monochromatic, with appropriate target choice as short as the laser pulse, and rather straightforward to produce. However, its brightness is very small due to isotropic emission and a lack of appropriate X-ray optics. In addition, polarization control and continuous tuning is not possible.

In summary, we have demonstrated an all optically driven undulator-radiation source. Ultrashort monochromatic electron pulses with energies around 60 MeV are produced by the interaction of a high-intensity laser with a gas jet. These electrons propagate through a static undulator of 2-cm period length and generate synchrotron radiation in the visible wavelength regime. This experiment marks an important step toward the application of high-intensity laser accelerators in conventional accelerator science. With a further increase of electron energy and the consequent reduction of undulator wavelength into the UV and even soft X-ray region—and with a future successful generation of coherent undulator radiation with the same method—this novel radiation source will be a valuable tool for a number of applications currently dependent on large free-electron laser installations like time-resolved X-ray imaging, diffraction, or microscopy.

ACKNOWLEDGMENT

The authors would like to thank B. Beleites, F. Ronneberger, and W. Ziegler for their technical support.

REFERENCES

[1] A. Zewail, "Femtochemistry: Atomic-scale dynamics of the chemical bond using ultrafast lasers," in *Nobel Lecture*, 1999.

[2] Y. J. Yan, B. Kohler, R. E. Gillilan, R. M. Whitnell, K. R. Wilson, and S. Mukamel, "Molecular control spectrometer," in *Ultrafast Phenomena VIII*, J.-L. Martin, A. Migus, and G. A. Mourou, Eds. Berlin, Germany: Springer-Verlag, 1993, pp. 8–12.

[3] H. Rabitz, R. de Vivie-Riedle, M. Motzkus, and K. Kompa, "Whither the future of controlling quantum phenomena?" *Science*, vol. 288, no. 5467, pp. 824–828, May 2000.

[4] D. H. Bilderback, P. Elleaume, and E. Weckert, "Review of third and next generation synchrotron light sources," *J. Phys. B, At. Mol. Opt. Phys.*, vol. 38, no. 9, pp. S773–S797, May 2005.

[5] F. Schotte, M. Lim, T. A. Jackson, A. V. Smirnov, J. Soman, J. S. Olson, G. N. Phillips, M. Wulff, and P. A. Anfinrud, "Watching a protein as it functions with 150-ps time-resolved X-ray crystallography," *Science*, vol. 300, no. 5627, pp. 1944–1947, Jun. 2003.

[6] H. Ihee, M. Lorenc, T. K. Kim, Q. Y. Kong, M. Cammarata, J. H. Lee, S. Bratos, and M. Wulff, "Ultrafast x-ray diffraction of transient molecular structures in solution," *Science*, vol. 309, no. 5738, pp. 1123–1227, Aug. 2005.

[7] V. Ayvazyan, N. Baboi, J. Bahr, V. Balandin, B. Beutner, A. Brandt, I. Bohnet, A. Bolzmann, R. Brinkmann, O. I. Brovko, J. P. Carneiro, S. Casalbuoni, M. Castellano, P. Castro, L. Catani, E. Chiadroni, S. Choroba, A. Cianchi, H. Delsim-Hashemi, G. Di Pirro, M. Dohlus, S. Dusterer, H. T. Edwards, B. Faatz, A. A. Fateev, J. Feldhaus, K. Flottmann, J. Frisch, L. Frohlich, T. Garvey, U. Gensch, N. Golubeva, H. J. Grabosch, B. Grigoryan, O. Grimm, U. Hahn, J. H. Han, M. V. Hartrott, K. Honkavaara, M. Huning, R. Ischebeck, E. Jaeschke, M. Jablonka, R. Kammering, V. Katalev, B. Keitel, S. Khodyachykh, Y. Kim, V. Kocharyan, M. Korfer, M. Kollewe, D. Kostin, D. Kramer, M. Krassilnikov, G. Kube, L. Lilje, T. Limberg, D. Lipka, F. Lohl, M. Luong, C. Magne, J. Menzel, P. Michelato, V. Miltchev, M. Minty, W. D. Moller, L. Monaco, W. Muller, M. Nagl, O. Napoly, P. Nicolosi, D. Nolle, T. Nunez, A. Oppelt, C. Pagani, R. Paparella, B. Petersen, B. Petrosyan, J. Pfluger, P. Piot, E. Plonjes, L. Poletto, D. Proch, D. Pugachov, K. Rehlich, D. Richter, S. Riemann, M. Ross, J. Rossbach, M. Sachwitz, E. L. Saldin, W. Sandner, H. Schlarb, B. Schmidt, M. Schmitz, P. Schmuser, J. R. Schneider, E. A. Schneidmiller, H. J. Schreiber, S. Schreiber, A. V. Shabunov, D. Sertore, S. Setzer, S. Simrock, E. Sombrowski, L. Staykov, B. Steffen, F. Stephan, F. Stulle, K. P. Sytchev, H. Thom, K. Tiedtke, M. Tischer, R. Treusch, D. Trines, I. Tsakov, A. Vardanyan, R. Wanzenberg, T. Weiland, H. Weise, M. Wendt, I. Will, A. Winter, K. Wittenburg, M. V. Yurkov, I. Zagorodnov, P. Zambolin, and K. Zapfe, "First operation of a free-electron laser generating gw power radiation at 32 nm wavelength," *Eur. Phys. J. D*, vol. 37, no. 2, pp. 297–303, Feb. 2006.

[8] H. N. Chapman, A. Barty, M. J. Bogan, S. Boutet, M. Frank, S. P. Hau-Riege, S. Marchesini, B. W. Woods, S. Bajt, W. H. Benner, R. A. London, E. Plönjes, M. Kuhlmann, R. Treusch, S. Dsterer, T. Tschentscher, J. R. Schneider, E. Spiller, T. Möller, C. Bostedt, M. Hoener, D. A. Shapiro, K. O. Hodgson, D. van der Spoel, F. Burmeister, M. Bergh, C. Caleman, G. Huldt, M. M. Seibert, F. R. N. C. Maia, R. W. Lee, A. Szöke, N. Timneanu, and J. Hajdu, "Femtosecond diffractive imaging with a soft-X-ray free-electron laser," *Nat. Phys.*, vol. 2, pp. 839–843, 2006.

[9] T. Tajima and J. M. Dawson, "Laser electron accelerator," *Phys. Rev. Lett.*, vol. 43, no. 4, pp. 267–270, 1979.

[10] E. Esarey, P. Sprangle, J. Krall, and A. Ting, "Overview of plasma-based accelerator concepts," *IEEE Trans. Plasma Sci.*, vol. 24, no. 2, pp. 252–288, Apr. 1996.

[11] M. Pittman, S. Ferré, J. Rousseau, L. Notebaert, J. P. Chambaret, and G. Chériaux, "Design and characterization of a near-diffraction-limited femtosecond 100-TW 10-Hz high-intensity laser system," *Appl. Phys. B, Lasers Opt.*, vol. 74, no. 6, pp. 529–535, Apr. 2002.

[12] A. Pukhov and J. Meyer-ter Vehn, "Laser wake field acceleration: The highly non-linear broken-wave regime," *Appl. Phys. B, Lasers Opt.*, vol. 74, no. 4/5, pp. 355–361, Apr. 2002.

[13] S. P. Mangles, C. D. Murphy, Z. Najmudin, A. G. Thomas, J. L. Collier, A. E. Dangor, E. J. Divall, P. S. Foster, J. G. Gallacher, C. J. Hooker, D. A. Jaroszynski, A. J. Langley, W. B. Mori, P. A. Norreys, F. S. Tsung, R. Viskup, B. R. Walton, and K. Krushelnick, "Monoenergetic beams of relativistic electrons from intense laser–plasma interactions," *Nature*, vol. 431, no. 7008, pp. 535–538, Sep. 2004.

[14] C. G. Geddes, C. S. Toth, J. van Tilborg, E. Esarey, C. B. Schroeder, D. Bruhwiler, C. Nieter, J. Cary, and W. P. Leemans, "High-quality electron beams from a laser wakefield accelerator using plasma-channel guiding," *Nature*, vol. 431, no. 7008, pp. 538–541, Sep. 2004.

[15] J. Faure, Y. Glinec, A. Pukhov, S. Kiselev, S. Gordienko, E. Lefebvre, J.-P. Rousseau, F. Burgy, and V. Malka, "A laser–plasma accelerator producing monoenergetic electron beams," *Nature*, vol. 431, no. 7008, pp. 541–544, Sep. 2004.

[16] W. P. Leemans, B. Nagler, A. J. Gonsalves, C. Toth, K. Nakamura, C. G. R. Geddes, E. Esarey, C. B. Schroeder, and S. Hooker, "GeV electron beams from a centimetre-scale accelerator," *Nat. Phys.*, vol. 2, pp. 696–699, 2006.

[17] J. van Tilborg, C. B. Schroeder, C. V. Filip, C. Toth, C. G. Geddes, G. Fubiani, R. Huber, R. A. Kaindl, E. Esarey, and W. P. Leemans, "Temporal characterization of femtosecond laser–plasma-accelerated electron bunches using terahertz radiation," *Phys. Rev. Lett.*, vol. 96, no. 1, p. 014 801, Jan. 2006.

[18] H.-P. Schlenvoigt, K. Haupt, A. Debus, F. Budde, O. Jackel, S. Pfotenhauer, H. Schwoerer, E. Rohwer, J. G. Gallacher, E. Brunetti, R. P. Shanks, S. M. Wiggins, and D. A. Jaroszynski, "A compact synchrotron radiation source driven by a laser–plasma wakefield accelerator," *Nat. Phys.*, vol. 4, no. 2, pp. 130–133, Feb. 2008.

[19] B. Hidding, K. U. Amthor, B. Liesfeld, H. Schwoerer, S. Karsch, M. Geissler, L. Veisz, K. Schmid, J. G. Gallacher, S. P. Jamison, D. Jaroszynski, G. Pretzler, and R. Sauerbrey, "Generation of quasi-monoenergetic electron bunches with 80-fs laser pulses," *Phys. Rev. Lett.*, vol. 96, no. 10, p. 105 004, Mar. 2006.

[20] H. Schwoerer, B. Liesfeld, H. P. Schlenvoigt, K. U. Amthor, and R. Sauerbrey, "Thomson-backscattered X-rays from laser-accelerated electrons," *Phys. Rev. Lett.*, vol. 96, no. 1, p. 014 802, Jan. 2006.

[21] K. A. Tanaka, T. Yabuuchi, T. Sato, R. Kodama, Y. Kitagawa, T. Takahashi, T. Ikeda, Y. Honda, and S. Okuda, "Calibration of imaging plate for high energy electron spectrometer," *Rev. Sci. Instrum.*, vol. 76, no. 1, p. 013 507, Jan. 2005.

[22] Y. Glinec, J. Faure, A. Guemnie-Tafo, V. Malka, H. Monard, J. P. Larbre, V. De Waele, J. L. Marignier, and M. Mostafavi, "Absolute calibration for a broad range single shot electron spectrometer," *Rev. Sci. Instrum.*, vol. 77, no. 10, p. 103 301, Oct. 2006.

[23] D. T. Attwood, *Soft X-Rays and Extreme Ultraviolet Radiation*. Cambridge, U.K.: Cambridge Univ. Press, 2000.

[24] J. A. Clarke, *The Science and Technology of Undulators and Wigglers*. Oxford, U.K.: Oxford Science, 2004.

[25] J. Faure, C. Rechatin, A. Norlin, A. Lifschitz, Y. Glinec, and V. Malka, "Controlled injection and acceleration of electrons in plasma wakefields by colliding laser pulses," *Nature*, vol. 444, no. 7120, pp. 737–739, Dec. 2006.

[26] Y. Glinec, J. Faure, A. Norlin, A. Pukhov, and V. Malka, "Observation of fine structures in laser-driven electron beams using coherent transition radiation," *Phys. Rev. Lett.*, vol. 98, no. 19, p. 194 801, May 2007.

[27] D. A. Jaroszynski, P. Chaix, N. Piovella, D. Oepts, G. M. H. Knippels, A. F. G. vanderMeer, and H. H. Weits, "Superradiance in a short-pulse free-electron-laser oscillator," *Phys. Rev. Lett.*, vol. 78, no. 9, pp. 1699–1702, Mar. 1997.

[28] J. Feldhaus, J. Arthur, and J. B. Hastings, "X-ray free-electron lasers," *J. Phys. B, At. Mol. Opt. Phys.*, vol. 38, no. 9, pp. S799–S819, May 2005.

[29] F. Gruner, S. Becker, U. Schramm, M. Fuchs, R. Weingartner, D. Habs, J. Meyer-Ter-Vehn, M. Geissler, M. Ferrario, L. Serafini, B. Van Der Geer, H. Backe, W. Lauth, and S. Reiche, "Design considerations for table-top, laser-based vuv and X-ray free electron lasers," *Appl. Phys. B, Lasers Opt.*, vol. 86, no. 3, pp. 431–435, Feb. 2007.

[30] D. Jaroszynski, R. Bingham, E. Brunetti, B. Ersfeld, J. Gallacher, B. van der Geer, R. Issac, S. Jamison, D. Jones, M. de Loos, A. Lyachev, V. Pavlov, A. Reitsma, Y. Saveliev, G. Vieux, and S. Wiggins, "Radiation sources based on laser–plasma interactions," *Philos. Trans. Roy. Soc. London A, Math. Phys. Sci.*, vol. 364, no. 1840, pp. 689–710, Mar. 2006.

[31] H. Schwoerer, P. Gibbon, S. Dusterer, R. Behrens, C. Ziener, C. Reich, and R. Sauerbrey, "MeV X-rays and photoneutrons from femtosecond laser-produced plasmas," *Phys. Rev. Lett.*, vol. 86, no. 11, pp. 2317–2320, Mar. 2001.

[32] F. Ewald, H. Schwoerer, and R. Sauerbrey, "K_α-radiation from relativistic laser-produced plasmas," *Europhys. Lett.*, vol. 60, no. 5, pp. 710–716, Dec. 2002.

[33] B. M. Hegelich, B. J. Albright, J. Cobble, K. Flippo, S. Letzring, M. Paffett, H. Ruhl, J. Schreiber, R. K. Schulze, and J. C. Fernandez, "Laser acceleration of quasi-monoenergetic MeV ion beams," *Nature*, vol. 439, no. 7075, pp. 441–444, Jan. 2006.

[34] H. Schwoerer, S. Pfotenhauer, O. Jackel, K. U. Amthor, B. Liesfeld, W. Ziegler, R. Sauerbrey, K. W. D. Ledingham, and T. Esirkepov, "Laser-plasma acceleration of quasi-monoenergetic protons from microstructured targets," *Nature*, vol. 439, no. 7075, pp. 445–448, Jan. 2006.

[35] A. Rousse, K. T. Phuoc, R. Shah, A. Pukhov, E. Lefebvre, V. Malka, S. Kiselev, F. Burgy, J. P. Rousseau, D. Umstadter, and D. Hulin, "Production of a KeV X-ray beam from synchrotron radiation in relativistic laser–plasma interaction," *Phys. Rev. Lett.*, vol. 93, no. 13, p. 135 005, 2004.

[36] K. T. Phuoc, S. Corde, R. Shah, F. Albert, R. Fitour, J. P. Rousseau, F. Burgy, B. Mercier, and A. Rousse, "Imaging electron trajectories in a laser-wakefield cavity using betatron X-ray radiation," *Phys. Rev. Lett.*, vol. 97, no. 22, p. 225 002, Dec. 2006.

[37] P. Catravas, E. Esarey, and W. P. Leemans, "Femtosecond X-rays from Thomson scattering using laser wakefield accelerators," *Meas. Sci. Technol.*, vol. 12, no. 11, pp. 1828–1834, Oct. 2001.

[38] T. Feurer, A. Morak, I. Uschmann, C. Ziener, H. Schwoerer, E. Forster, and R. Sauerbrey, "An incoherent sub-picosecond X-ray source for timeresolved X-ray-diffraction experiments," *Appl. Phys. B, Lasers Opt.*, vol. 72, no. 1, pp. 15–20, Jan. 2001.

Hans-Peter Schlenvoigt was born 1981. He received the Diploma degree in physics with a diploma thesis on Thomson Backscattering from relativistic laser-accelerated electrons from the University of Jena, Germany, in 2005, where he is currently working toward the Ph.D. degree.

During the Ph.D. degree, he continued working within the field of electron acceleration from high-intensity laser plasma. During the synchrotron-radiation experiment, he was, on behalf of H. Schwoerer, the Organizer of all experimental work done at Jena.

Kerstin Haupt, photograph and biography not available at the time of publication.

Alexander Debus, photograph and biography not available at the time of publication.

Fabian Budde, photograph and biography not available at the time of publication.

Oliver Jäckel, photograph and biography not available at the time of publication.

Sebastian Pfotenhauer, photograph and biography not available at the time of publication.

Jordan G. Gallacher, photograph and biography not available at the time of publication.

Enrico Brunetti, photograph and biography not available at the time of publication.

Richard P. Shanks, photograph and biography not available at the time of publication.

Samuel M. Wiggins, photograph and biography not available at the time of publication.

Dino A. Jaroszynski, photograph and biography not available at the time of publication.

Erich Rohwer, photograph and biography not available at the time of publication.

Heinrich Schwoerer was born in 1964. He received the Diploma degree in physics with a thesis in low-temperature solid state physics from the University of Heidelberg, Heidelberg, Germany, in 1999 and the Ph.D. degree with a dissertation in physical chemistry from the Swiss Federal Institute of Technology, Zurich, Switzerland, in 1994.

During a first postdoctoral fellowship, he was working on coherent control of molecular dynamics at Wuerzburg. Since 1999, he has been with the Institut fuer Optik und Quantenelektronik, Friedrich-Schiller-Universität Jena, Jena, Germany, where he started his research activities in relativistic laser plasma physics with emphasis on particle acceleration and generation of high-energy radiation with lasers. Since 2007, he has also been holding the South African Research Chair on photonics and ultrafast and ultraintense laser science with the Laser Research Institute, University of Stellenbosch (RSA), Matieland, South Africa.